

NUCLEAR RAINBOWS, NUCLEUS–NUCLEUS
POTENTIALS AND THE EOS OF NUCLEAR MATTER*W. VON OERTZEN[†], H.G. BOHLEN

Hahn Meitner Institut, Glienickerstr. 100, 14109 Berlin, Germany

V. SUBOTIN

Nuclear Physics Department, St. Petersburg University
Ulianovskaja 1, 198904 St. Petersburg, Russia

AND DAO T. KHOA

Institute for Nuclear Science, VAEC, P.O.Box 5T-160, Hanoi, Vietnam

(Received December 17, 2001)

The elastic scattering of strongly bound nuclei at energies of 7–70 MeV/ u shows the phenomenon of Rainbow Scattering. These scattering processes are due to strongly attractive potentials leading to deflections to negative angles and involve a strong overlap of nuclear densities. The elastic scattering of $^{16}\text{O}+^{16}\text{O}$ has been studied in several laboratories over a wide range of energies with high precision to very low cross sections at large angles. At high energy the systematics of the primary Airy maxima has been established and at lower energies higher order Airy-structures are identified. The angular distributions at all energies are consistently described with *deep* potentials, as obtained from the double-folding model with a weakly density dependent effective nucleon–nucleon interaction, which gives in Hartree-Fock calculations a soft ($K=230$ MeV) equation of state for cold nuclear matter. It is shown that the Pauli-blocking expected for the larger density overlaps at small energies is strongly reduced due to the large relative momenta of the two centres in a self-consistent treatment of the mean field effects, the Fermi-spheres of the two nuclei in the overlap region are strongly repelled in momentum space, due to the increase of the relative momenta of nucleons. The systematics of the data also confirms the refractive origin of structures in one-neutron transfer reactions, as well as the pronounced structure in the excitation functions in $^{16}\text{O}+^{16}\text{O}$ scattering observed at lower energies.

PACS numbers: 21.30.Fe, 25.70.Bc, 24.10.Ht

* Presented at the XXVII Mazurian Lakes School of Physics, Krzyże, Poland, September 2–9, 2001.

[†] Also at Fachbereich Physik, Freie Universität, Berlin.

1. Rainbow scattering

The rainbow observed in nature with the sunlight occurs due to a particular sequence of refractions and reflections and an unusual systematic behaviour of the total “deflection angle”. We have one *refraction* when light enters the water-droplet (see Fig. 1), one *reflection* inside and a *second refraction* when the light leaves the droplet. The rainbow appears as a strongly enhanced region of light followed by a “shadow”. The unusual nature of this phenomenon has been recognised for the first time by Descartes in 1637, when he published his book *Les Meteores*.

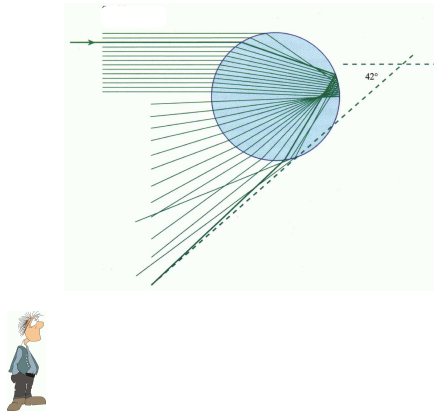


Fig. 1. The deflection of light (from the sun) entering the water droplet at different impact parameters with two refractions and one reflection, which are responsible for the rainbow phenomenon with a maximum deflection angle at $(180^\circ - 138^\circ) = 42^\circ$, the rainbow angle θ_R .

The peculiar interest for the physicists in the rainbow phenomenon is not the colour splitting connected to the broad spectrum of wavelength in the sun, but the fact that more light intensity is observed at the rainbow angle of 42° , where classically a singularity for the intensity would occur, followed by a dark region at larger angles [1, 2]. The secondary rainbow often observed in nature, is produced by a second reflection inside the droplet, due to this circumstance the ordering of the colours is then reversed as compared to the primary rainbow.

2. Nuclear rainbow scattering

Refractive nuclear (rainbow) scattering has been the subject of increased attention in the last decades, because it has been established that deep potentials are needed to describe the systematics of light heavy ion scattering. Originally (20–30 years ago) the data for many light heavy ion systems at

lower energies were fitted with rather shallow potentials. However, the recent studies [3], in particular for the $^{16}\text{O}+^{16}\text{O}$ scattering [4–7, 9, 10] as well as for α -particle scattering [11, 12], with the use of the new double-folding model produced very deep real parts of the optical potential. The work of the last decade has focused attention to the high energy data of light heavy ion scattering, where a unique determination of the real potential has become possible. These new precise and complete data for differential cross sections for elastic scattering of $^{16}\text{O}+^{16}\text{O}$, extending over seven orders of magnitude (two to three orders further down than previous data!), revealed a very clear *sensitivity of the large angle scattering on the details of the real potential at small distances*. At these small distances, where large density overlaps of the scattered nuclei occur, the potential as obtained from the double-folding model is very sensitive to the details of the effective nucleon–nucleon interaction (based *e.g.* on the Paris M3Y-interaction [5, 13, 14]). Thus it has been shown that a consistent description can only be obtained with a distinct, but small density dependence in the NN -interaction [5, 9, 13, 14]. We note that for these collisions the survival probability of the projectile passing through the target nucleus is in the range of 0.1%, this is expressed by the S -matrix elements shown in Fig. 2. The well defined elastic scattering “projects out” from the many channels, the channel with the ground states of the two nuclei. The corresponding data points are located at large scattering angles and have to be measured with high accuracy.

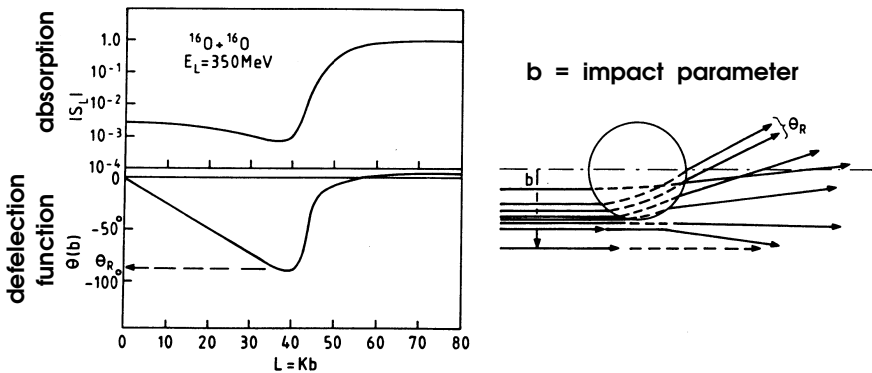


Fig. 2. The deflection function (angle variation as function of angular momentum L , or impact parameter (b), in the $^{16}\text{O}+^{16}\text{O}$ scattering at $E_{\text{lab}}=350$ MeV, leading to negative angles with the maximum deflection at the rainbow angle θ_R . The simultaneous absorption probability is shown in form of the absolute value of the S -Matrix elements. The refraction occurs due to the attractive nuclear potential, the position of the rainbow angle θ_R depends on the strength of the potential and the kinetic energy of the particles, or on their wavelength. This angle would define the limits of the shadow and light regions, however, the intensity around this angle varies in a particular way (Airy structures) as shown in Fig. 3.

The refined methods developed for the double-folding model are concerned with a correct treatment of the non-local exchange part of the potential and the new density dependent effective nucleon–nucleon interactions (BDM3Y), which give the correct saturation point of nuclear matter in Hartree–Fock calculations [14]. The systematics of all refractive scattering data favours a weak density dependence and a *soft* equation of state of cold nuclear matter [10, 12–14], with an incompressibility parameter in the range of $K \simeq 220\text{--}250$ MeV (with an accuracy of $(\pm 15\%)$).

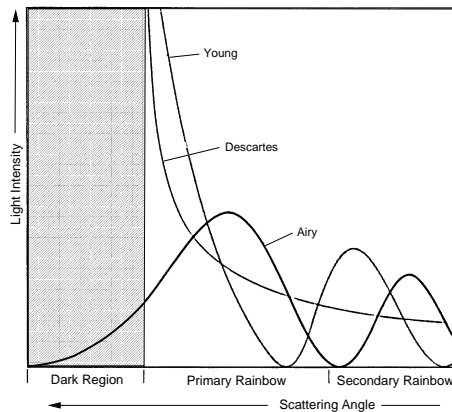


Fig. 3. The Airy function describing the rainbow phenomenon. The first intensity maximum appears within the classical lighted region away from the classical sharp shadow border line. The scattered intensity extends into the dark region and in the lighted region higher order Airy-maxima and -minima occur. These are indeed observed in $^{16}\text{O}+^{16}\text{O}$ scattering at lower energy, see Figs. 4 and 5. The “classical” solutions (like Descartes and Young) show divergence of the intensity around the rainbow angle θ_R .

3. The $^{16}\text{O}+^{16}\text{O}$ system

We give a brief survey of the recent experimental results for the elastic scattering of $^{16}\text{O}+^{16}\text{O}$ over a wide range of energies. Precise data have now been measured up to large angles for low energies at IreS in the range of $E_{\text{lab}} = 75\text{--}124$ MeV (at 9 energies [6]), and at energies $E_{\text{lab}} = 250, 350, 480, 704$ and 1120 MeV at the HMI and at GANIL [7]; further data at two energies have been measured by Sugiyama *et al.* [8]. It is very important for the conclusions from this work to have high quality data over the whole angular range. Previous data seldom extended over this large range, and the measurement of the new data needed quite an experimental effort.

Fig. 4 shows the result for the elastic scattering at the higher energies (124 MeV up to 1120 MeV), and separately data at the lower energies. The elastic scattering data have been fitted with an optical potential, where the real part has been obtained by the double-folding model or by a functional dependence of Woods–Saxon squared form $f_i^2(r)$, where $f_i(r) = (1 + \exp(\frac{r-R_i}{a_i}))^{-1}$; with $i = V, W$ for the real and imaginary parts. The latter parametrisation gives potential shapes, which are very close to the double-folding potentials. In addition a surface term, with a form factor of the derivative, $4a_S \frac{d}{dr} f_S(r)$ has to be added to the imaginary potential, as has been found already in earlier work [14].

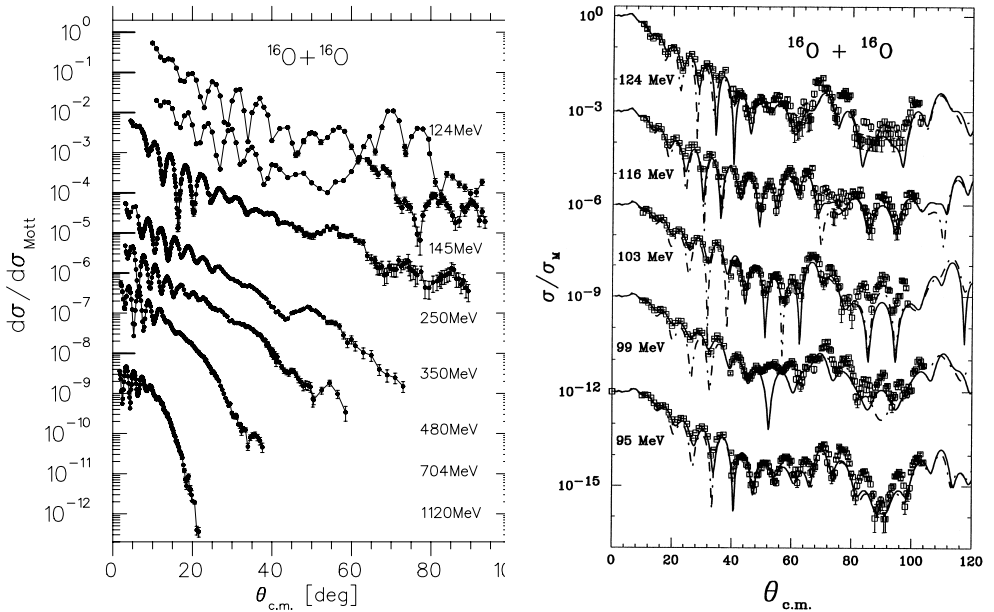


Fig. 4. Differential cross section of $^{16}\text{O} + ^{16}\text{O}$ elastic scattering over many energies (the fits to these data are discussed in Refs. [6, 7]). Left panel: for energies $E_{\text{lab}} = 124$ to 1120 MeV. The primary rainbow maximum at $E_{\text{lab}} = 350$ MeV is located at an angle of 55° , it moves to larger angles outside the observation region at lower energies, and for higher energies to smaller angles, *e.g.* to 10° at 1120 MeV. Right panel: Differential cross sections at energies between $E_{\text{lab}} = 95$ and 124 MeV [6], with curves calculated with optical model potentials obtained from the double-folding model or with the Woods–Saxon squared potentials.

We repeat here the basic facts (see Figs. 2 and 3) of rainbow scattering [2, 3]. The rainbow structure appears if the nuclear potential is strong enough to deflect particles into “negative angles”, and a maximum deflection (rainbow) angle occurs. In this case a particular oscillating interference

structure due to contributions from several impact parameters contributing to the maximum deflection angle will appear, which is described by an Airy-function (this function is shown in Fig. 3). The higher order maxima, which are referred to as 2nd/3rd-*etc.*, order Airy structures, will appear inside the “lighted” region. Note that the “secondary” rainbow (with the reversed colours) in nature is due to a second reflection inside of the droplet, whereas the 2nd Airy maximum is usually barely seen as opposed to the nuclear rainbow scattering.

The most remarkable feature of this complete data set (Fig. 4) for $^{16}\text{O} + ^{16}\text{O}$, is the fact that we can follow the evolution of the primary and secondary Airy-structures from the energies of $E_{\text{lab}} = 350$ MeV, where the 1st maximum is very pronounced, up to 1 GeV, where the primary rainbow has moved into the diffractive region, and down to 124 MeV and lower, where only the *higher order Airy structures* appear in the angular range of observation.

The situation with respect to the Airy structures can be shown, see Fig. 5, if we make a calculation for the near-far-side decomposition and *without symmetrisation*. The result is shown together with the experimental data for the case of $E_{\text{lab}} = 124$ MeV. At this energy the 3rd Airy maximum appears at an angle of 72° .

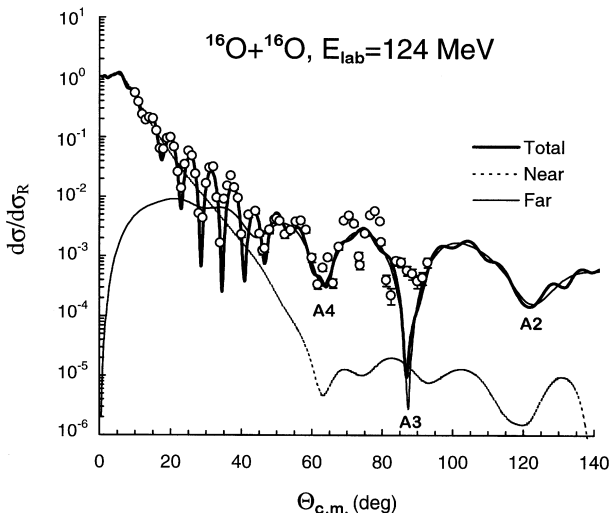


Fig. 5. Calculations and data illustrating the occurrence of higher order Airy structures (minima marked by A_i , $i = 2-4$). The calculations show the near/far-side decomposition and have *no symmetrisation* for the identity of the two ^{16}O nuclei. The data show the additional oscillations due to the interference of the identical amplitudes for spin zero bosons.

In the systematic measurements also data [17, 18] have been obtained for the one-neutron transfer reaction $^{16}\text{O}(^{16}\text{O}, ^{17}\text{O})^{15}\text{O}$, populating the ground ($p1/2$ -hole) and first excited state of ^{15}O , the ($p3/2$ -hole)-state. The one-neutron form factor now emphasises different radial regions of the scattering potentials. Thus it is quite important to state, that indeed at the rainbow angles a distinct maximum is observed also in this channel, as shown in Fig. 6, for those energies, where the primary rainbow maximum has been observed. The final fit shown in the figure needed an increased absorption for the $^{17}\text{O}+^{15}\text{O}$ -channel, a feature which is consistent with our understanding of absorption in heavy ion scattering. In this combination of nuclei with ^{17}O more channels are open, and the particle-“hole” in the closed shell nucleus ^{16}O forming states in ^{15}O leads to a faster decay of the “cluster” inside the medium, just like a broken piece of sugar dissolves faster in a liquid. With the double folding model potential it was possible to describe the data at all energies with one normalisation for the product of the spectroscopic factors [17, 18] .

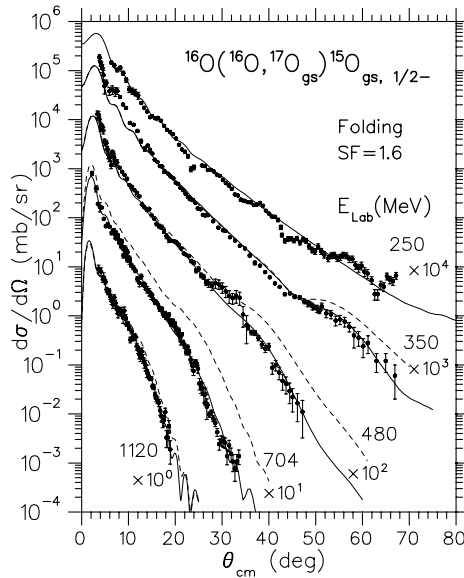


Fig. 6. Data for the one neutron transfer illustrating the occurrence of refractive structures for reactions. The calculations show the result of DWBA calculations with the real potentials from the double-folding model, and a constant product of spectroscopic factors (SF). For the imaginary part in the exit channel two choices are shown, dashed curve — same potentials as the entrance channel, full curve — increased absorption in the $^{17}\text{O}+^{15}\text{O}$ -channel.

4. Double folding model and the EOS of nuclear matter

In the systematic analysis of the elastic scattering data over many energies with the double-folding model or with potentials with shapes chosen to be the Woods–Saxon squared (WS2) form [6, 7] it was found, that both give equivalent overall fits to the data. We must emphasise the most important point concerning these “new” potentials : *The originally (30 years ago) used Wood-Saxon potentials have the wrong radial shapes* and thus fail to reproduce the systematics over many energies. Many cases of α -particle scattering have also been analysed in the last 15 years in a systematic way, and it has been established that the deep potentials of the cited shapes are needed, to describe scattering states *and* bound states consistently [15].

For further discussion the potentials can be classified by their volume integrals defined as

$$J_{V,W} = -\frac{4\pi}{N_A N_B} \int V_{V,W}(r) r^2 dr, \quad (1)$$

which are normalised to the number of interacting nucleon pairs (nucleon numbers are given by N_A and N_B for projectile and target). Already in previous studies using the double-folding model [14] for the nucleus–nucleus potentials, in particular for α -particle-nucleus scattering [11, 12], it has been found that a consistent description is obtained with particular values of the volume integral for nucleon–nucleus potentials [3]. These values vary little for different systems, thus a criterion for the choice of the potentials for composite systems has often been a consistent value of the volume integral of the real potential per interacting nucleon pair.

Our result for the real potentials is also consistent with other results for composite particles, the values for the volume integrals which are obtained [3, 6, 7] are typically $J_V \simeq 300 \text{ MeV fm}^3$ at $E_{\text{lab}} \simeq 30 \text{ MeV}/u$. The volume integrals of heavier particles are slightly reduced due to antisymmetrisation effects. We will come back to this question later. The systematics of these volume integrals are shown for $^{16}\text{O}+^{16}\text{O}$ in Fig. 7 over all energies.

An important aspect of the analysis of refractive scattering has been the study of the in-medium effective nucleon–nucleon interaction [10, 12–14]. This is achieved by introducing into the M3Y-interaction a density dependence in such a way that the corresponding Hartree–Fock calculation reproduces the saturation point of nuclear matter [9, 10, 14, 16, 19]. In the double-folding model *and* in the Hartree–Fock calculation the exchange part (which is non-local) must be treated consistently. In this approach also the systematics of the nucleon–nucleus potentials as well as the mean field potentials of nucleons as obtained by Jeukenne *et al.* [19] are well reproduced [14]. In the Hartree–Fock calculations different choices of the

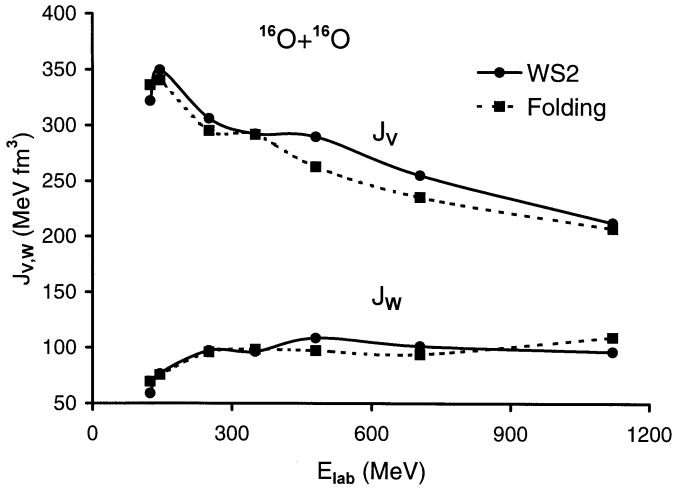


Fig. 7. Volume integrals J_V , and J_W of the real and imaginary part, respectively, of the best-fit real WS2 and the folded potentials for the $^{16}\text{O}+^{16}\text{O}$ system at incident energies from $E_{\text{lab}} = 124\text{--}1120$ MeV. The lines are only to guide the eye.

density dependence give different values of the nuclear incompressibility, described by the factor K . Examples of such calculations for the equation of state (EOS) with different values of K are given in Fig. 8.

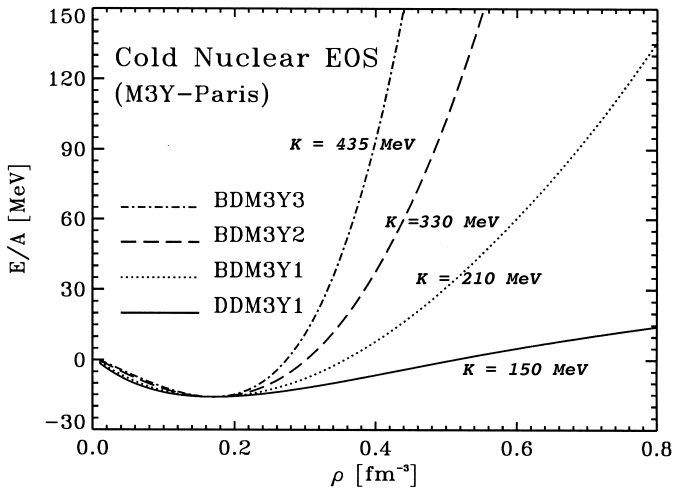
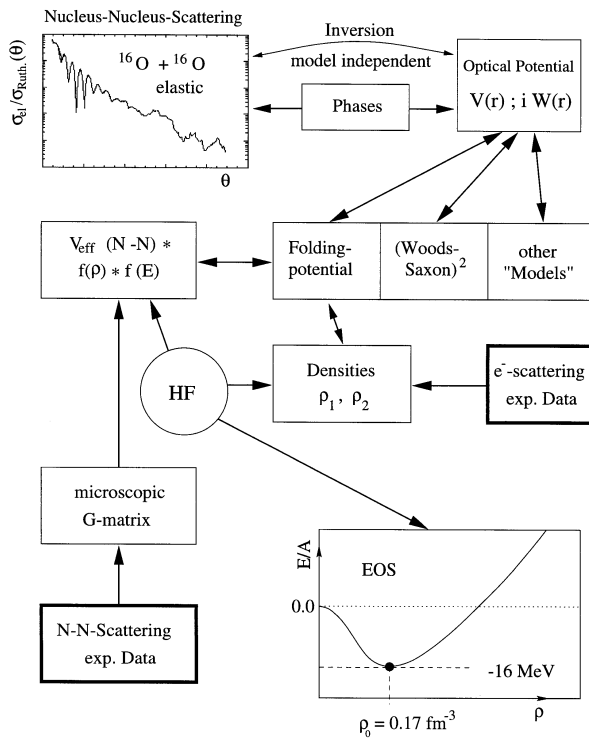


Fig. 8. Results of Hartree–Fock calculations using different versions of the density dependent M3Y(Paris) interaction, giving different values for the incompressibility constant K , but the same saturation point of nuclear matter.

An interesting observation is made in a different study of light ion scattering in Ref. [21]; in their analysis the nucleon–nucleon interaction of Ref. [19] has been chosen, restricting the folding procedure to normal nuclear densities without the superposition of the two densities. The analysis fails to reproduce the pronounced rainbow structures for all the cases, where the experiments extend to the larger angles! The present double-folding model with the density dependent (BDM3Y) nucleon–nucleon interaction and the local density approximation with the density pile-up has now been used in many other systems including the scattering of weakly bound radioactive ions.

Experimental Data



Equation of State

Fig. 9. Connection between various experimental data for nucleus–nucleus elastic scattering, nucleon–nucleon scattering and electron–nucleus scattering for the determination of the nucleus–nucleus potentials. In the analysis enter the nuclear densities, the effective nucleon–nucleon interaction, and finally due to the Hartree–Fock calculations with different versions of the density dependent M3Y(Paris) N – N -interaction, giving the correct saturation point of nuclear matter, different values for the incompressibility constant K .

At this point it is worth to give an overview over the experimental and theoretical input into the description of the nucleus–nucleus scattering with the Double Folding Model (DFM), (see Fig. 9). Once the parameters of the Hartree–Fock calculations are fixed, reproducing the proper saturation point (as shown in Fig. 8), the remaining parameters, which are needed for the nuclear densities are determined from experimental results (electron scattering) and reproduced analytically by using appropriate shell model wave functions. In Fig. 9 the connections between the different inputs are illustrated. For the determination of the EOS of nuclear matter, the nucleus–nucleus potential can also be obtained from a model independent analysis [9, 10, 17] of the data, in this case the experimental errors are transformed into an error band for the potential. This potential is then reproduced by the DFM, for which a single normalisation constant, typically in the range of 0.75 to 0.9 depending on energy, is introduced. The data for α -particle scattering [16] turned out to show the strongest sensitivity on the compressibility constant, there pronounced nuclear rainbows have been observed since 30 years.

5. Consideration of Pauli-blocking and conclusions

Finally we come back to the question of the Pauli-blocking effects in the double-folding model (DFM) which predicts in both, heavy ion scattering and α -particle scattering, very deep potentials (which can also be closely reproduced by a Woods–Saxon-squared shape). The experimental systematics of the elastic scattering data down to the lowest energies as shown Fig. 4, imply that the DFM seems still to be applicable at the lower energies. This is in contradiction with the Pauli-blocking effect expected to be strong if large density overlap occurs at low energies. The double folding model with an effective N – N -interaction adjusted to the properties of nuclear matter, gives a potential for the elastic channel as *a mean field effect*, which is indeed very deep in accordance with the cited empirical result. The deep potentials, which are observed could be seen to comply with the Pauli principle by generating the appropriate number of nodes for the wave function in the interior (according to the rule that $(2N + L) = \sum(n_i + l_i)$ as discussed in Ref. [8]).

We note that also a self-consistent description of the exchange part of the potential, which is non-local, has been very important in the new concept of double-folding model [13, 14]. In more recent work we have now shown in Ref. [20], that the inclusion of the Pauli-blocking in the double folding also can be done in a self-consistent way. This has been formulated in a Pauli Distorted Double Folding Model (PDDFM), where the semi-classical Thomas–Fermi approach is used. The main idea, as explained in Ref. [20], is shown in Fig. 10. Due to the fact that the value of the relative momen-

tum of the nucleons in the two nuclei, which enters into the calculations, is determined by a very deep double folding (mean field) potential, its value effectively increases strongly once the self-consistent description of the local potentials is used. Therefore, the overlap between the two Fermi-spheres in momentum space is reduced, and thus the Pauli-blocking diminishes strongly in the regions of strong spatial overlap. The potentials remain deep even in the energy range down to 6-10MeV/nucleon, although with some small renormalisation as discussed in Ref. [20]. The Pauli-distortion of the wave functions of the nuclei described in this reference, actually will lead to excitations of the nuclei and to absorption from the elastic channel (known as Pauli-excitation in atomic physics). However, these distortions have to be transformed into discrete quantal excitations of the fragments, these are partially suppressed for strongly bound nuclei, which have no states at low excitation energies like in ^{16}O or for α -particles.

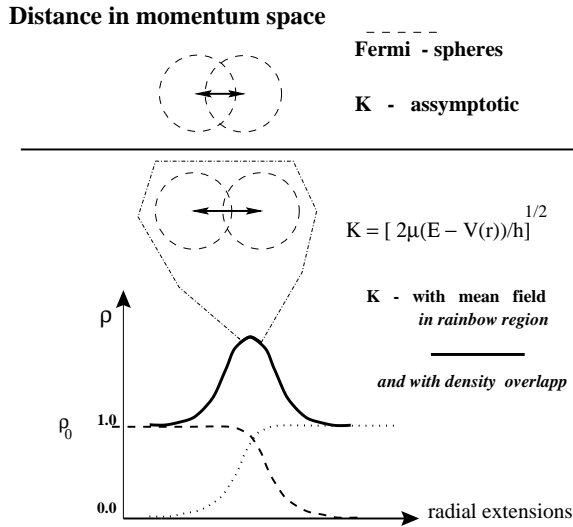


Fig. 10. Illustration of the reduction of the Pauli-blocking. The local momentum \mathbf{K} of nucleons during the overlap of the densities must be determined self-consistently with the very strong attractive potential created simultaneously. In rainbow scattering large overlaps of densities with values up to twice the saturation value (ρ_0) are observed in the elastic channel. A “repulsion” of the nucleonic Fermi-spheres thus occurs due to a self-consistent mean field effect in the double-folding model.

We can thus understand the systematics of nuclear rainbow scattering and their associated real potentials down to rather low energies of 7 MeV/nucleon and even lower. At these low energies the deep potential creates the observed interference patterns in the angular distributions, which are due to 3rd/4th and higher order Airy structures. The older studies of

low energy elastic scattering in the $^{12}\text{C}+^{12}\text{C}$ and $^{16}\text{O}+^{16}\text{O}$ systems appear in a completely new light. The structures observed in these systems for the excitation functions of the elastic cross section at 90° are due to the passage of the steep Airy-minima as function of energy, described as “Airy-elephants” in Ref. [3]. Very pronounced rainbow structures are also observed in recent precise data for the elastic scattering in the $^{16}\text{O}+^{12}\text{C}$ system [22]. The double-folding method and the BDM3Y interaction are also now used in many cases for the analysis of scattering systems with weakly bound radioactive beams [23].

In conclusion we find, that the complete set of data for the $^{16}\text{O}+^{16}\text{O}$ system gives clear criteria for the choice of a particular class of real potentials, which agree well with the results of the double-folding model calculations, based on a nucleon–nucleon interaction with a weak density dependence as discussed in Refs. [5, 9, 10, 12–14]. The result of the double-folding model is also consistent with our knowledge on the nucleon–nucleon interaction, on measured nuclear densities and with the saturation properties of nuclear matter. The related scattering trajectories for the elastic channel are deeply penetrating, creating an appreciable density overlap of the two nuclei. Thus the refractive scattering of strongly bound nuclei is one of the clearest sources on information related to the in-medium nucleon–nucleon interaction and the compressibility of nuclear matter. We repeat here the statement, that the S -matrix elements leading to the rainbow angles are in the range of 0.1%, thus high precision data at large angles are needed to obtain such results.

This work has been partially supported by the German Ministry of Research (BMFT, Verbundforschung, under contract: 06OB472D/4).

REFERENCES

- [1] W. von Oertzen, D.T. Khoa, H.G. Bohlen, *Europhys. News* **31/2**, 5 (2000) and **31/3**, 21 (2000).
- [2] J.D. Jackson, *Phys. Rep.* **320**, 27 (1999).
- [3] M.E. Brandan, G.R. Satchler, *Phys. Rep.* **285**, 143 (1997).
- [4] H.G. Bohlen, E. Stiliaris, B. Gebauer *et al.*, *Z. Phys.* **A346**, 189 (1993).
- [5] D.T. Khoa, W. von Oertzen *et al.*, *Phys. Rev. Lett.* **74**, 34 (1995).
- [6] M.P. Nicoli, F. Haas, R.M. Freeman, *et al.*, *Phys. Rev.* **C60**, 064608 (1999).
- [7] Dao T. Khoa, W. von Oertzen, H.G. Bohlen, *et al.*, *Nucl. Phys.* **A672**, 387 (2000).
- [8] Y. Kondo, Y. Sugiyama *et al.*, *Phys. Lett.* **B365**, 17 (1996).
- [9] G. Bartnitzky *et al.*, *Phys. Lett.* **B365**, 23 (1996).

- [10] G. Bartnitzky *et al.*, *Phys. Lett.* **B386**, 7 (1996).
- [11] S. Ohkubo, *Phys. Rev. Lett.* **74**, 2176 (1995).
- [12] D.T. Khoa, W. von Oertzen, *Phys. Lett.* **B342**, 6 (1995).
- [13] D.T. Khoa, W. von Oertzen, H.G. Bohlen, *Phys. Rev.* **C49**, 1652 (1994).
- [14] D.T. Khoa, W. von Oertzen, *Phys. Lett.* **B304**, 8 (1993).
- [15] F. Michel, S. Ohkubo, G. Reidemeister, *Progr. Theor. Suppl.* **132**, 7 (1998).
- [16] D.T. Khoa, G.R. Satchler, W. von Oertzen, *Phys. Rev.* **C56**, 954 (1997).
- [17] F. Nouffer, Thesis 2001, University of Tuebingen.
- [18] H.G. Bohlen *et al.*, submitted to *Nucl. Phys.* **A**.
- [19] J.P. Jeukenne, A. Lejeune, C. Mahaux, *Phys. Rev.* **C16**, 80 (1977).
- [20] V. Subbotin, W. von Oertzen *et al.*, *Phys. Rev.* **C64**, 014601-1 (2001).
- [21] L. Trache, A. Azhari, H.L. Clark *et al.*, *Phys. Rev.* **C61** 024612-1 (2000).
- [22] A.A. Ogloblin, Yu.A. Glukhov, W.H. Trzarska *et al.*, *Phys. Rev.* **C62**, 044601-1 (2000) and references therein.
- [23] M. Avrigeanu, G.S. Anagnostatos, A.N. Antonov, J. Giapitzakis, *Phys. Rev.* **C62**, 017001 (2000); M. Avrigeanu, A.N. Antonov, H. Lenske, I. Şteţcu, *Nucl. Phys.* **A693**, 616 (2001).